

Full Length Research Paper

Similarity solution of hydromagnetic heat and mass transfer over a vertical plate with a convective surface boundary condition

O. D. Makinde

Faculty of Engineering, Cape Peninsula University of Technology, P. O. Box 1906, Bellville 7535, South Africa.
E-mail: makinded@cput.ac.za.

Accepted 25 May, 2010

This paper examined the hydromagnetic boundary layer flow with heat and mass transfer over a vertical plate in the presence of magnetic field and a convective heat exchange at the surface with the surrounding has been studied. The similarity solution is used to transform the system of partial differential equations, describing the problem under consideration, into a boundary value problem of coupled ordinary differential equations and an efficient numerical technique is implemented to solve the reduced system. A comparison study with the previous results shows a very good agreement. The results are presented graphically and the conclusion is drawn that the flow field and other quantities of physical interest are significantly influenced by these parameters.

Key words: Vertical plate, convective boundary condition, heat and mass transfer, magnetic field, similarity solution.

INTRODUCTION

Magneto-hydrodynamic (MHD) boundary layers with heat and mass transfer over flat surfaces are found in a many engineering and geophysical applications such as geothermal reservoirs, thermal insulation, enhanced oil recovery, packed-bed catalytic reactors, cooling of nuclear reactors. Many chemical engineering processes like metallurgical and polymer extrusion processes involve cooling of a molten liquid being stretched into a cooling system; the fluid mechanical properties of the penultimate product depend mainly on the cooling liquid used and the rate of stretching. Some polymer fluids like Polyethylene oxide and polyisobutylene solution in cetane, having better electromagnetic properties, are normally used as cooling liquid as their flow can be regulated by external magnetic fields in order to improve the quality of the final product. A comprehensive review on the subject of the above problem has been made by many researchers (Yang et al., 1982; Trevisan and Bejan, 1990; Sparrow et al., 1962; Evans, 1962). The similarity solutions for hydromagnetic mixed convection heat and mass transfer for Hiemenz flow through porous media as

explained by Chamkha and Khaled (2000). Postelnicu (2004) numerically studied the influence of magnetic field on heat and mass transfer by natural convection from vertical surfaces in porous media by considering the Soret and Dufour effects. Makinde (2005) carried out a numerical study on the effect of thermal radiation on boundary layer flow with heat and mass transfer past a moving vertical porous plate. Seddeek (2001) studied the thermal radiation and buoyancy effects on MHD free convection heat generation flow over an accelerating permeable surface with temperature dependent viscosity.

Ghaly and Seddeek (2004) investigated the effects of chemical reaction, heat and mass transfer on laminar flow along a semi infinite horizontal plate with temperature dependent viscosity. The effect of thermal radiation on heat and mass transfer flow of a variable viscosity fluid past a vertical porous plate permeated by a transverse magnetic field was reported in Makinde and Ogulu (2008). Recently Aziz (2009) reported a similarity solution for laminar thermal boundary layer over a flat plate with a convective surface boundary condition. The paper demonstrates that a similarity solution is possible if the convective heat transfer associated with the hot fluid on the lower surface of the plate is proportional to the

Abbreviation: MHD, Magneto-hydrodynamic.

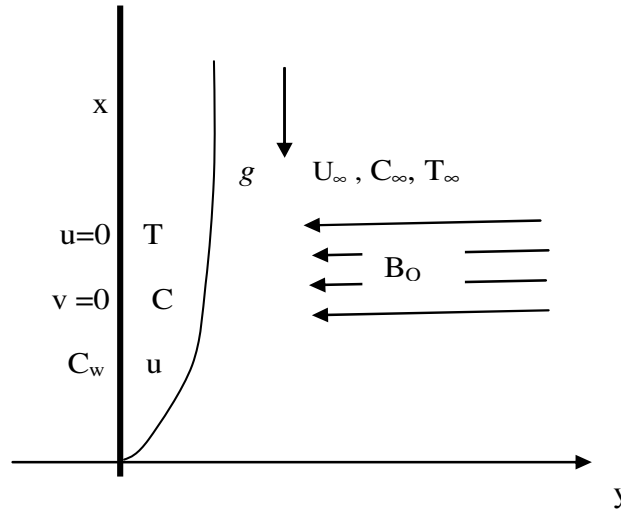


Figure 1. Flow configuration and coordinate system.

inverse square root of the axial distance.

Hence, the purpose of the present work is to extend the recent work of Aziz (2009) to include hydromagnetic mixed convection heat and mass transfer over a vertical plate with a convective surface boundary condition. The governing boundary-layer equations have been transformed to a two-point boundary value problem in similarity variables, and these have been solved numerically. The effects of magnetic field, Prandtl number, Schmidt number, Grashof number and convective heat transfer parameter on fluid velocity, temperature and concentration have been shown graphically. It is hoped that the results obtained will not only provide useful information for applications, but also serve as a complement to the previous studies.

MATHEMATICAL MODEL

Let us consider a steady, laminar, hydromagnetic coupled heat and mass transfer by mixed convection flow over a vertical plate. The fluid is assumed to be Newtonian, electrically conducting and its property variations due to temperature and chemical species concentration are limited to fluid density. The density variation and the effects of the buoyancy are taken into account in the momentum equation (Boussinesq approximation). In addition, there is no applied electric field and all of the Hall effects and Joule heating are neglected (Figure 1). Since the magnetic Reynolds number is very small for most fluid used in industrial applications, we assume that the induced magnetic field is negligible.

Let the x-axis be taken along the direction of plate and y-axis normal to it. If u , v , T and C are the fluid x-component of velocity, y-component of velocity, temperature and concentration respectively, then under the Boussinesq and boundary-layer approximations, the governing equations for this problem can be written as:

$$\frac{\partial u}{\partial x} + \frac{\partial v}{\partial y} = 0, \quad (1)$$

$$u \frac{\partial u}{\partial x} + v \frac{\partial u}{\partial y} = \nu \frac{\partial^2 u}{\partial y^2} - \frac{\sigma B_0^2}{\rho} (u - U_\infty) + g \beta_T (T - T_\infty) + g \beta_c (C - C_\infty), \quad (2)$$

$$u \frac{\partial T}{\partial x} + v \frac{\partial T}{\partial y} = \alpha \frac{\partial^2 T}{\partial y^2}, \quad (3)$$

$$u \frac{\partial C}{\partial x} + v \frac{\partial C}{\partial y} = D \frac{\partial^2 C}{\partial y^2}, \quad (4)$$

where ν is the kinematic viscosity, T_∞ is the free stream temperature, C_∞ is the free stream concentration, U_∞ is the free stream velocity, α is the thermal diffusivity and D is the mass diffusivity, β_T is the thermal expansion coefficient, β_c is the solutal expansion coefficient, ρ is the fluid density, g is gravitational acceleration and σ is the fluid electrical conductivity.

The boundary conditions at the plate surface and far into the cold fluid may be written as

$$\begin{aligned} u(x,0) &= v(x,0)=0, & -k \frac{\partial T}{\partial y}(x,0) &= h[T - T_w(x,0)], \\ C_w(x,0) &= Ax^\lambda + C_\infty, \\ u(x,\infty) &= U_\infty, \quad T(x,\infty) = T_\infty, \quad C(x,\infty) = C_\infty, \end{aligned} \quad (5)$$

where h is the plate heat transfer coefficient, L is the plate characteristic length, C_w is the species concentration at the plate surface, λ is the plate surface concentration exponent and k is the thermal conductivity coefficient. The stream function ψ , satisfies the continuity Equation (1) automatically with

$$u = \frac{\partial \psi}{\partial y} \quad \text{and} \quad v = -\frac{\partial \psi}{\partial x}. \quad (6)$$

A similarity solution of Equations (1) – (6) is obtained by defining an

independent variable η and a dependent variable f in terms of the stream function ψ as

$$\eta = y \sqrt{\frac{U_\infty}{\nu x}}, \quad \psi = \sqrt{\nu x U_\infty} f(\eta). \quad (7)$$

The dimensionless temperature and concentration are given as

$$\theta(\eta) = \frac{T - T_\infty}{T_w - T_\infty}, \quad \phi(\eta) = \frac{C - C_\infty}{C_w - C_\infty}. \quad (8)$$

where T_w is the temperature of the hot fluid at the left surface of the plate. Substituting Equations (6) - (8) into Equations (1) - (5), we obtain

$$f''' + \frac{1}{2} f f'' - Ha_x (f' - 1) + Gr_x \theta + Gc_x \phi = 0, \quad (9)$$

$$\theta'' + \frac{1}{2} Pr f \theta' = 0, \quad (10)$$

$$\phi'' + \frac{1}{2} Sc f \phi' = 0, \quad (11)$$

$$f(0) = 0, f'(0) = 0, \theta'(0) = Bi_x [\theta(0) - 1], \phi(0) = 1, \quad (12)$$

$$f'(\infty) = 1, \theta(\infty) = \phi(\infty) = 0, \quad (13)$$

where the prime symbol represents the derivative with respect to η and

$$Ha_x = \frac{\sigma B_0^2 x}{\rho U_\infty} \quad (\text{the Magnetic field parameter}),$$

$$Gr_x = \frac{g \beta_T (T_w - T_\infty) x}{U_\infty^2} \quad (\text{the thermal Grashof number}),$$

$$Gc_x = \frac{g \beta_c (C_w - C_\infty) x}{U_\infty^2} \quad (\text{the solutal Grashof number}),$$

$$Bi_x = \frac{h}{k} \sqrt{\frac{\nu x}{U_\infty}} \quad (\text{Convective heat transfer parameter}),$$

$$Pr = \frac{\nu}{\alpha} \quad (\text{the Prandtl number}),$$

$$Sc = \frac{\nu}{D} \quad (\text{the Schmidt number}).$$

It is noteworthy that the local parameters Bi_x , Ha_x , Gr_x and Gc_x in

Equations (9) - (13) are functions of x . However, in order to have a similarity solution all the parameters Bi_x , Ha_x , Gr_x , Gc_x must be constant and we therefore assume

$$h = cx^{\frac{1}{2}}, \sigma = ax^{\frac{1}{2}}, \beta_T = bx^{\frac{1}{2}}, \beta_c = dx^{\frac{1}{2}}. \quad (14)$$

where a , b , c , d are constants.

Other physical quantities of interest in this problem such as the skin friction parameter $\tau = f'(0)$, the plate surface temperature $\theta(0)$,

Nusselt number $Nu = -\theta'(0)$ and the Sherwood number

$Sh = -\phi'(0)$ can be easily computed. For local similarity case, integration over the entire plate is necessary to obtain the total skin friction, total heat and mass transfer rate.

NUMERICAL PROCEDURE

The system of non-linear ordinary differential equations (9) - (11) with boundary conditions (12) - (13) have been solved numerically by using the Runge-Kutta integration scheme with a modified version of the Newton-Raphson shooting method with Bi_x , Ha_x , Gr_x , Gc_x , Sc and Pr as prescribed parameters. The computations were done by a program which uses a symbolic and computational computer language MAPLE (Heck, 2003). A step size of $\Delta\eta = 0.001$ was selected to be satisfactory for a convergence criterion of 10^{-7} in nearly all cases. The value of η_∞ was found to each iteration loop by the assignment statement $\eta_\infty = \eta_\infty + \Delta\eta$. The maximum value of η_∞ , to each group of parameters with Bi_x , Ha_x , Gr_x , Gc_x , Sc and Pr is determined when the values of unknown boundary conditions at $\eta = 0$ not change to successful loop with error less than 10^{-7} .

RESULTS AND DISCUSSION

The governing equations (9) - (11) subject to the boundary conditions (12) - (13) are integrated as described in Section 3. Numerical results are reported in the Tables 1 - 2 and Figures 2 - 10. The Prandtl number was taken to be $Pr = 0.72$ which corresponds to air, the values of Schmidt number (Sc) were chosen to be $Sc = 0.24, 0.62, 0.78, 2.62$, representing diffusing chemical species of most common interest in air like H_2 , H_2O , NH_3 and Propyl Benzene respectively. Attention is focused on positive values of the buoyancy parameters that is, Grashof number $Gr_x > 0$ (which corresponds to the cooling problem) and solutal Grashof number $Gc_x > 0$ (which indicates that the chemical species concentration in the free stream region is less than the concentration at the boundary surface). In order to benchmark our numerical results, we have compared the plate surface temperature $\theta(0)$ and the local heat transfer rate at the plate surface $\theta'(0)$ in the absence of both magnetic field and buoyancy forces for various values of Bi with those of Aziz (2009) and found them in excellent agreement as demonstrated in Table 1. From Table 2, it is important to

Table 1. Computations showing comparison with Aziz [11] results for $Ha_x = 0$, $Gr_x = Gc_x = 0$, $Pr = 0.72$ and $Sc = 0.63$.

Bi_x	$\theta(0)$ Aziz (2009)	$-\theta'(0)$ Aziz (2009)	$\theta(0)$ Present	$-\theta'(0)$ Present
0.05	0.1447	0.0428	0.14466	0.04276
0.10	0.2528	0.0747	0.25275	0.07472
0.20	0.4035	0.1193	0.40352	0.11929
0.40	0.5750	0.1700	0.57501	0.16999
0.60	0.6699	0.1981	0.66991	0.19805
0.80	0.7302	0.2159	0.73016	0.21586
1.00	0.7718	0.2282	0.77182	0.22817
5.00	0.9441	0.2791	0.94417	0.27913
10.00	0.9713	0.2871	0.97128	0.28714
20.00	0.9854	0.2913	0.98543	0.29132

Table 2. Computation showing $f''(0)$, $\theta(0)$, $\phi'(0)$ and $\theta'(0)$ for various values of embedded parameter $Pr = 0.72$.

Bi_x	Gr_x	Gc_x	Ha_x	Sc	$f''(0)$	$-\theta'(0)$	$\theta(0)$	$-\phi'(0)$
0.1	0.1	0.1	0.1	0.24	0.62601	0.07707	0.22929	0.21859
1.0	0.1	0.1	0.1	0.24	0.68213	0.25501	0.74498	0.22169
10	0.1	0.1	0.1	0.24	0.70577	0.33335	0.96666	0.22296
0.1	0.5	0.1	0.1	0.24	0.72193	0.07760	0.22393	0.22381
0.1	1.0	0.1	0.1	0.24	0.83124	0.07815	0.21849	0.22937
0.1	0.1	0.5	0.1	0.24	1.12789	0.07969	0.20306	0.24852
0.1	0.1	1.0	0.1	0.24	1.66664	0.08143	0.18562	0.27339
0.1	0.1	0.1	1.0	0.24	1.13812	0.07875	0.21244	0.23452
0.1	0.1	0.1	5.0	0.24	2.30247	0.08034	0.19652	0.25077
0.1	0.1	0.1	0.1	0.62	0.60020	0.07677	0.23221	0.31232
0.1	0.1	0.1	0.1	0.78	0.59428	0.07671	0.23287	0.33955
0.1	0.1	0.1	0.1	2.62	0.56580	0.07641	0.23582	0.52053

note that the local skin friction together with the local heat and mass transfer rate at the plate surface increases with increasing intensity of buoyancy forces (Gr_x , Gc_x), magnetic field (Ha_x) and convective heat exchange parameter (Bi_x). However, an increase in the Schmidt number (Sc) causes a decrease in both skin friction and surface heat transfer rate and an increase in the surface mass transfer rate.

Effects of parameter variation on velocity profiles

The effects of various parameters on velocity profiles in the boundary layer are depicted in Figures 2 - 6. It is observed from Figures 2 - 6, that the velocity starts from a zero value at the plate surface and increases to the free stream value far away from the plate surface satisfying the far field boundary condition for all parameter values.

In Figure 2 the effect of increasing the magnetic field

strength on the momentum boundary-layer thickness is illustrated. It is now a well established fact that the magnetic field presents a damping effect on the velocity field by creating a drag force that opposes the fluid motion, causing the velocity to decrease. However, in this case an increase in the Ha_x only slightly slows down the motion of the fluid away from the vertical plate surface toward the free stream velocity, while the fluid velocity near the vertical plate surface increases. Similar trend of slight increase in the fluid velocity near the vertical plate is observed with an increase in convective heat transfer parameter Bi_x . Figures 4 and 5 show the variation of the boundary-layer velocity with the buoyancy forces parameters (Gr_x , Gc_x). In both cases an upward acceleration of the fluid in the vicinity of the vertical wall is observed with increasing intensity of buoyancy forces.

Further downstream of the fluid motion decelerates to the free stream velocity. Figure 6 shows a slight decrease in the fluid velocity with an increase in Schmidt number.

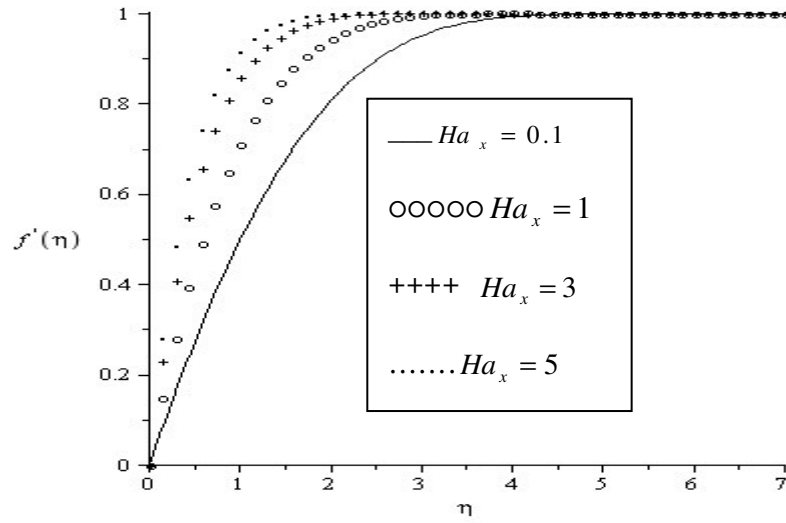


Figure 2. Velocity profile for $Pr=0.72$, $Sc=0.62$, $Gr_x=Gc_x=Bi_x=0.1$.

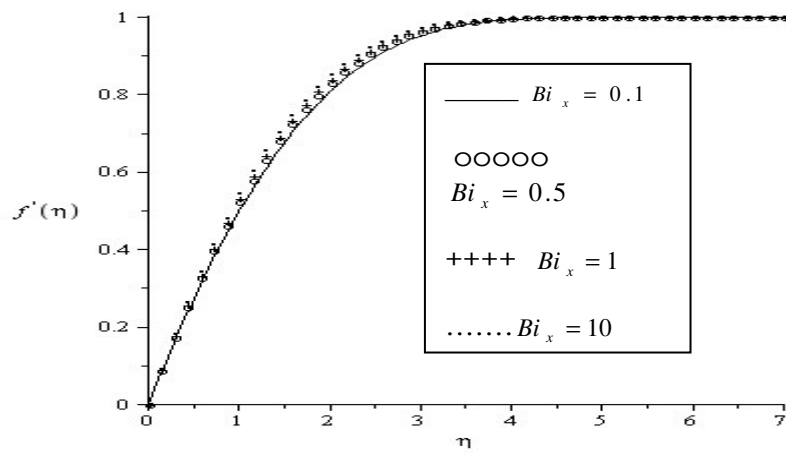


Figure 3. Velocity profile for $Pr=0.72$, $Sc=0.62$, $Gr_x=Gc_x=Ha_x=0.1$.

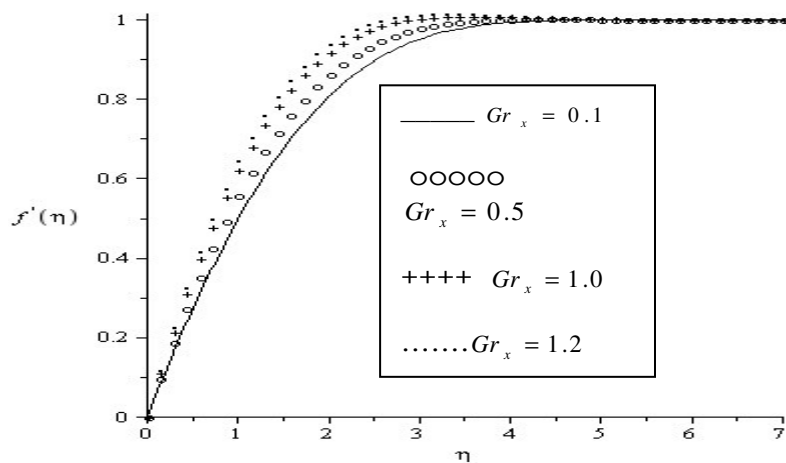


Figure 4. Velocity profiles for $Pr=0.72$, $Sc=0.62$, $Gc_x=Ha_x=Bi_x=0.1$.

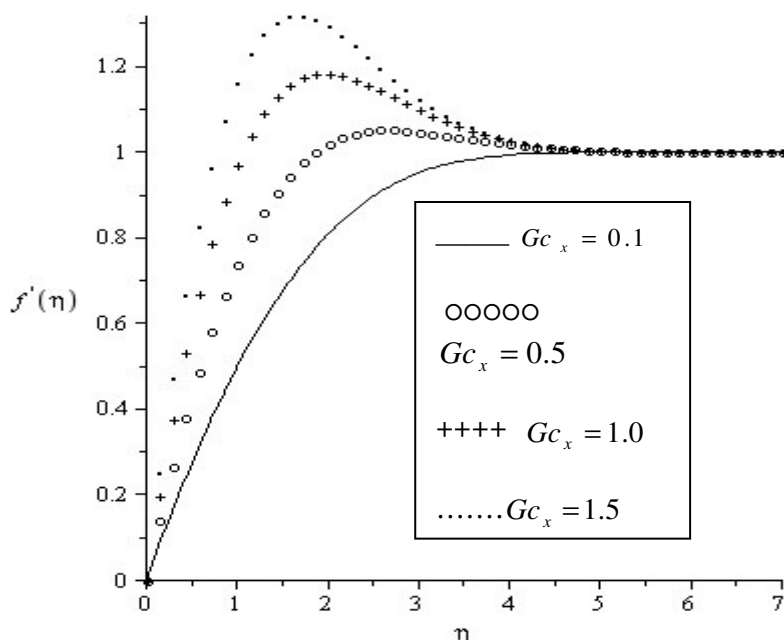


Figure 5. Velocity profiles for $Pr=0.72$, $Sc=0.62$, $Gr_x=Ha_x=Bi_x=0.1$.

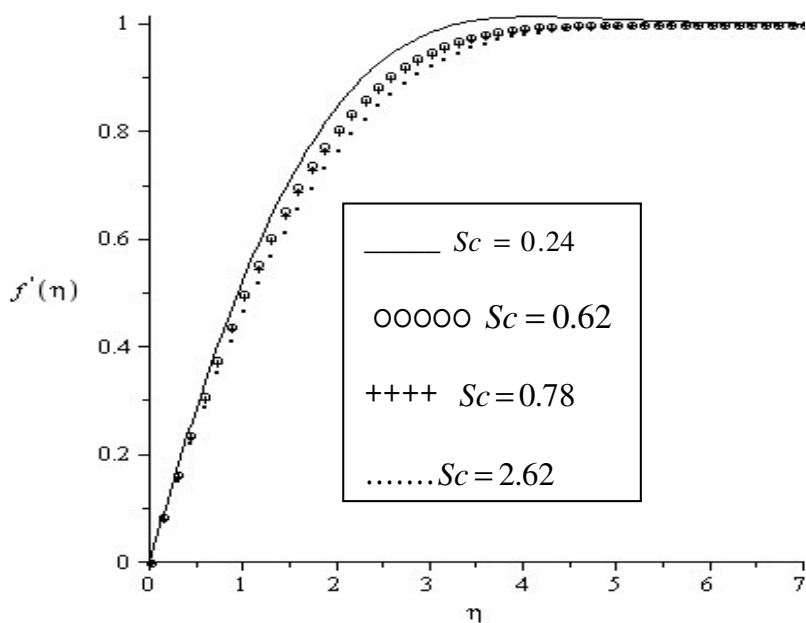


Figure 6. Velocity profiles for $Pr=0.72$, $Gr_x=Gc_x=Ha_x=Bi_x=0.1$.

Effects of parameter variation on temperature profiles

Generally, the fluid temperature attains its maximum value at the plate surface and decreases exponentially to the free stream zero value away from the plate satisfying the boundary condition. This is observed in Figures

7 - 11. From these figures, it is interesting to note that the thermal boundary layer thickness decreases with an increase in the intensity of magnetic field (Ha_x) and the buoyancy forces (Gr_x , Gc_x). Moreover, the fluid temperature increases with an increase in the Schmidt number (Sc) and the convective heat exchange at the plate surface (Bi_x) leading to an increase in thermal

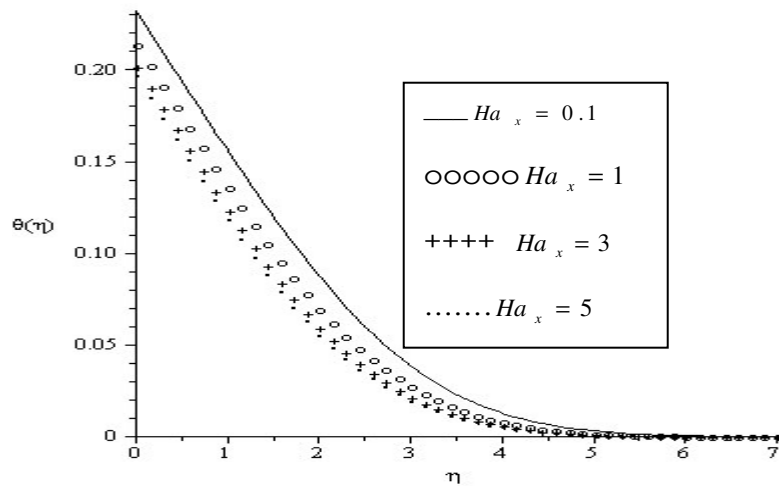


Figure 7. Temperature profiles for $Pr=0.72$, $Sc=0.62$, $Gr_x=Gc_x=Bi_x=0.1$.

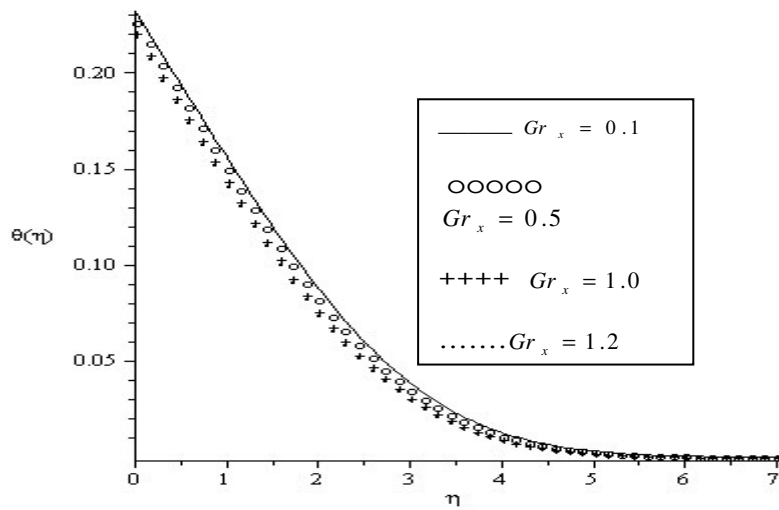


Figure 8. Velocity profiles for $Pr=0.72$, $Sc=0.62$, $Gc_x=Ha_x=Bi_x=0.1$.

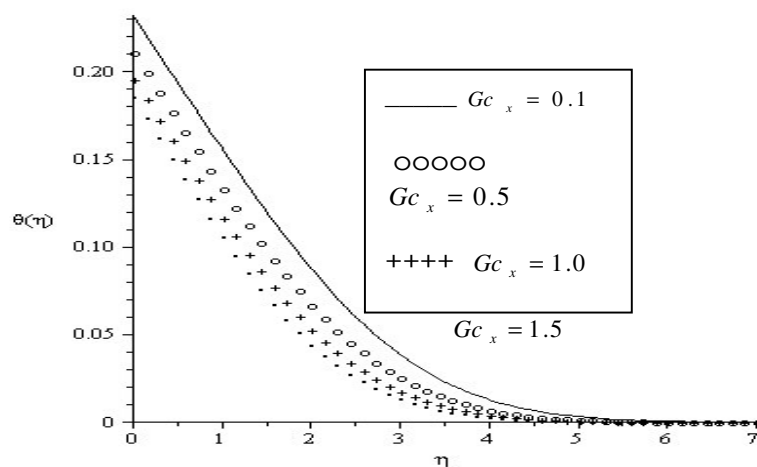


Figure 9. Temperature profile for $Pr=0.72$, $Sc=0.62$, $Gr_x=Ha_x=Bi_x=0.1$.

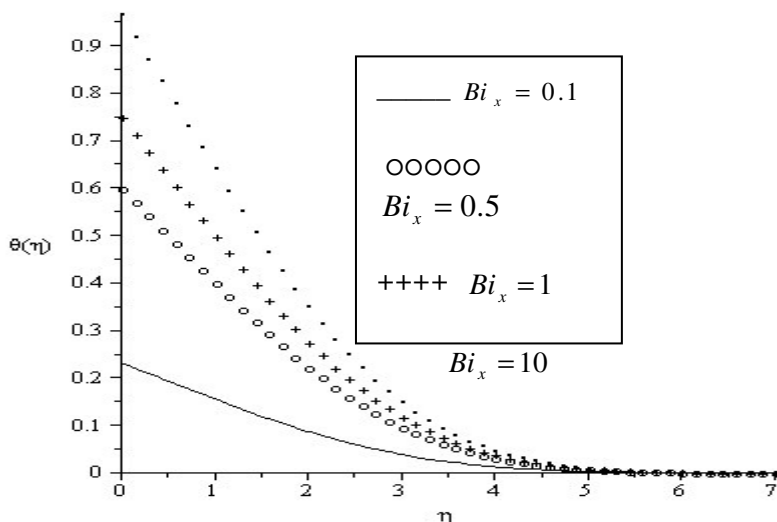


Figure 10. Temperature profiles for $Pr = 0.72$, $Sc = 0.62$, $Gr_x = Gc_x = Ha_x = 0.1$.

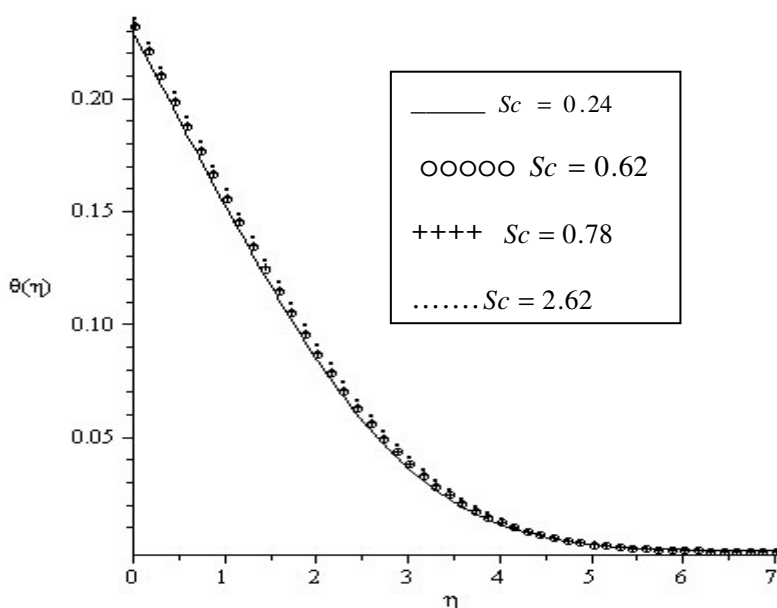


Figure 11. Temperature profile for $Pr = 0.72$, $Gr_x = Gc_x = Ha_x = Bi_x = 0.1$.

boundary layer thickness.

Effects of parameter variation on concentration profiles

Figures 12 – 14 depict chemical species concentration profiles against spanwise coordinate η for varying values physical parameters in the boundary layer. The species concentration is highest at the plate surface and decreases to zero far away from the plate satisfying the boundary condition. From these figures, it is noteworthy

that the concentration boundary layer thickness decreases with an increase in the magnetic field intensity (Ha_x). An increase in the values of solutal Grashof number due to buoyancy force and Schmidt number also causes a decrease in the chemical species concentration leading to a decaying concentration boundary layer thickness.

Conclusions

This paper studied hydromagnetic mixed convection heat

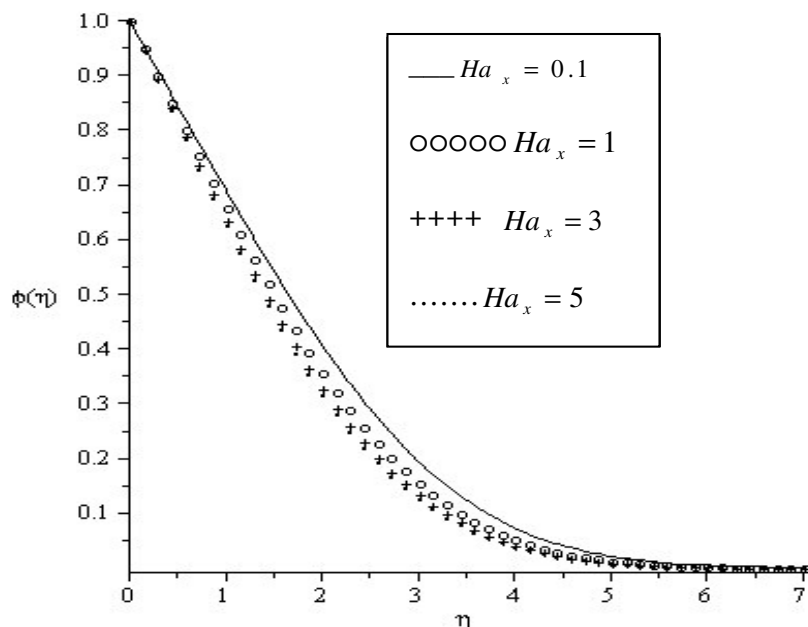


Figure 12. Concentration profiles for $Pr = 0.72$, $Sc = 0.62$, $Gr_x = Gc_x = Bi_x = 0.1$.

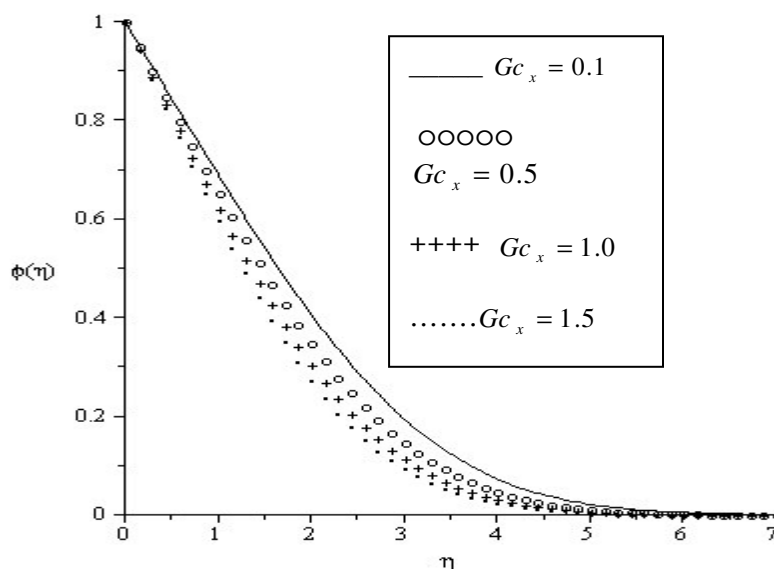


Figure 13. Concentration profiles for $Pr = 0.72$, $Sc = 0.62$, $Gr_x = Ha_x = Bi_x = 0.1$.

and mass transfer over a vertical plate subjected to convective heat exchange with the surrounding in the presence of magnetic field. The governing equations are approximated to a system of non-linear ordinary differential equations by similarity transformation. Numerical calculations are carried out for various values of the dimensionless parameters of the problem. A comparison with previously published work is performed and excellent agreement between the results is obtained. The results

are presented graphically and the conclusion is drawn that the flow field and other quantities of physical interest are significantly influenced by these parameters. The results for the prescribed skin friction, local heat and mass transfer rate at the plate surface are presented and discussed. It was found that the local skin-friction coefficient, local heat and mass transfer rate at the plate surface increases with an increase in intensity of magnetic field, buoyancy forces and convective heat

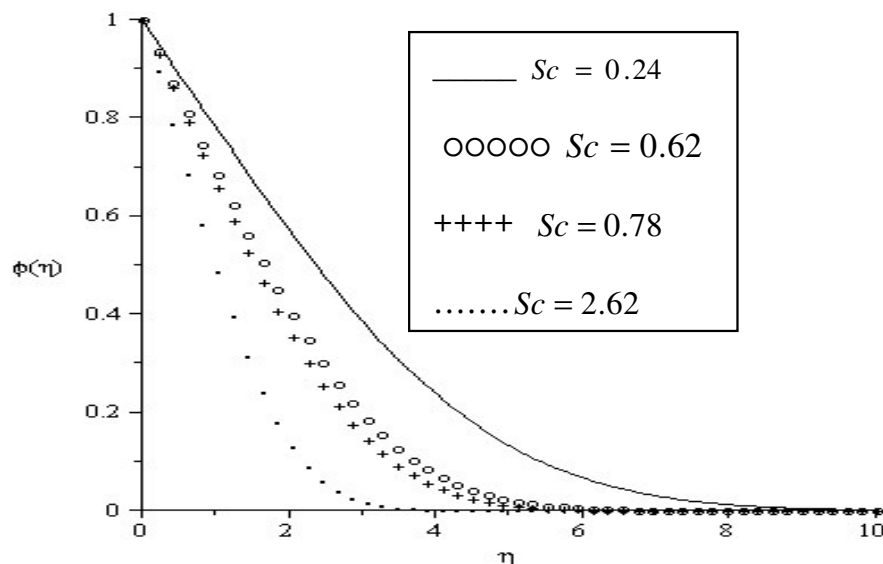


Figure 14. Concentration profiles for $Pr = 0.72$, $Gr_x = Gc_x = Bi_x = Ha_x = 0.1$.

exchange parameter.

ACKNOWLEDGEMENTS

The author would like to thank the anonymous referees for their useful suggestions and National Research Foundation of South Africa Thuthuka programme for financial support.

REFERENCES

- Aziz A (2009). A similarity solution for laminar thermal boundary layer over a flat plate with a convective surface boundary condition, *Commun. Nonlinear Sci. Numer. Simulat.* 14: 1064-1068.
- Chamkha AJ, Khaled AA (2000). Similarity solutions for hydromagnetic mixed convection heat and mass transfer for Hiemenz flow through porous media. *Int. J. Numer. Meth. Heat Fluid Flow* 10(1): 94-115.
- Evans HL (1962). Mass transfer through laminar boundary layers. *Int. J. Heat Mass Transfer* 5: 35-57.
- Ghaly AY, Seddeek MA (2004). Chebyshev finite difference method for the effects of chemical reaction, heat and mass transfer on laminar flow along a semi infinite horizontal plate with temperature dependent viscosity. *Chaos, Solitons Fract.* pp. 19-61.
- Heck A (2003). *Introduction to Maple*, 3rd Edition, Springer-Verlag.
- Makinde OD (2005). Free-convection flow with thermal radiation and mass transfer past a moving vertical porous plate, *Int. Comm. Heat Mass Transfer* 32: 1411-1419.
- Makinde OD, Ogulu A (2008). The effect of thermal radiation on the heat and mass transfer flow of a variable viscosity fluid past a vertical porous plate permeated by a transverse magnetic field, *Chem. Eng. Commun.* 195(12): 1575-1584.
- Postelnicu A (2004). Influence of a magnetic field on heat and mass transfer by natural convection from vertical surfaces in porous media considering Soret and Dufour effects, *Int. J. Heat Mass Transfer* 47: 1467-1472.
- Seddeek MA (2001). Thermal radiation and buoyancy effects on MHD free convection heat generation flow over an accelerating permeable surface with temperature dependent viscosity. *Canadian J. Phys.* 79: 725-732.
- Sparrow EM, Eckert ER, Minkowycz WJ (1962). Transpiration cooling in a magnetohydrodynamic stagnation-point flow, *Appl. Sci. Res. A* 11: 125-147.
- Trevisan OV, Bejan A (1990). Combined heat and mass transfer by natural convection in a porous medium, *Adv. Heat Transfer* 20: 315-352.
- Yang J, Jeng DR, DeWitt KJ (1982). Laminar Free Convection from a Vertical Plate with Non- uniform Surface Conditions, *Numer. Heat Transfer* 5: 165-184.

APPENDIX

Nomenclature		Greek symbols	
C_w	Plate surface concentration	η	Similarity variable
(u, v)	Velocity components	ψ	Stream function
(x, y)	Coordinates	θ	Dimensionless temperature
B_0	Magnetic field strength	μ	Dynamic viscosity
Gr_x	Thermal Grashof number	α	Thermal diffusivity
Pr	Prandtl number	β_T	Thermal expansion coefficient
P	Pressure	ν	Kinematic viscosity
g	Gravitational acceleration	ρ	Fluid density
Bi_x	Convective heat transfer parameter	β_c	Concentration expansion
	coefficient		
T_∞	Free stream temperature	ϕ	Dimensionless
	concentration		
C_∞	Free stream concentration	σ	Fluid electrical
	conductivity		
C_p	Specific heat capacity at constant pressure	ψ	Stream function
f	Dimensionless stream function		
U_∞	Free stream velocity		
Gc_x	Solutal Grashof number		